Neuropsychologia 48 (2010) 3743–3756

Contents lists available at ScienceDirect

Neuropsychologia

journal homepage: www.elsevier.com/locate/neuropsychologia

Adaptation modulates the electrophysiological substrates of perceived facial distortion: Support for opponent coding

Alex Burkhardt[a], Leslie M. Blaha[a,*], Bethany Schneider Jurs[b], Gillian Rhodes[c], Linda Jeffery[c], Dean Wyatte[a], Jordan DeLong[a], Tom Busey[a]

[a] Department of Psychological and Brain Sciences, Indiana University - Bloomington, Bloomington, IN 47405, United States
[b] Department of Psychology, University of Wisconsin - Stout, United States
[c] School of Psychology, The University of Western Australia, Australia

ARTICLE INFO

Article history:
Received 12 January 2010
Received in revised form 12 August 2010
Accepted 16 August 2010
Available online 21 August 2010

Keywords:
Face processing
Adaptation
Aftereffects
Event related potential

ABSTRACT

In two experiments we determined the electrophysiological substrates of figural aftereffects in face adaptation using compressed and expanded faces. In Experiment 1, subjects viewed a series of compressed and expanded faces. Results demonstrated that distortion systematically modulated the peak amplitude of the P250 event-related potential (ERP) component. As the amount of perceived distortion in a face increased, the peak amplitude of the P250 component decreased, regardless of whether the physical distortion was compressive or expansive. This provided an ERP metric of the degree of perceived distortion. In Experiment 2, we examined the effects of adaptation on the P250 amplitude by introducing an adapting stimulus that affected the subject's perception of the distorted test faces as measured through normality judgments. The set of test faces was held constant and the adapting stimulus was systematically varied across experimental days. Adapting to a compressed face made a less compressed test face appear more normal and an expanded test face more distorted as measured by normality ratings. We found that the adaptation conditions that increased the perceived distortion of the distorted test faces also decreased the amplitude of the P250. Likewise, adaptation conditions that decreased the perceived distortion of the distorted test faces also increased the amplitude of the P250. The results demonstrate that perceptual adaptation to compressed or expanded faces affected not only the behavioral normality judgments but also the electrophysiological correlates of face processing in the window of 190–260 ms after stimulus onset.

Adaptation techniques can be used to isolate neurophysiological mechanisms that are responsible for representing a stimulus. Through extended exposure, the adaptation procedure recalibrates the encoding mechanisms that respond in the presence of an adapting stimulus, resulting in systematic distortions of the perceptions of related stimuli, known as aftereffects. Adaptation aftereffects can alter the perception of subsequent stimuli in multiple ways. For example, adaptation to a distorted image can make a similarly distorted image appear more undistorted, while adaptation to the same distorted image can make an image distorted in an opposite direction appear more distorted. Aftereffects based on the perception of an object's shape are termed *figural aftereffects* (Gibson, 1933; Köhler & Wallach, 1944).

An illustrative example of these patterns can be found in studies of faces, where the use of adaptation procedures has proven useful to explore both the mechanisms for encoding face information and the temporal organization of those mechanisms. For example, Webster and MacLin (1999) demonstrated that perceptual adaptation to a compressed or expanded face caused a test face to appear distorted in the direction opposite to the adapting face. They showed that if one were to adapt to an expanded face, a normal test face would appear more compressed and an expanded face would appear more normal. Webster and MacLin (1999) termed this pattern of findings the *face figural aftereffect*, because it was based on the distortion of spatial or figural information within the adapting and test faces. Similar results have been found for *identity aftereffects* (Leopold, O'Toole, Vetter, & Blanz, 2001) in which adaptation to a particular identity alters the perceived identities of other faces. Strong aftereffects also occur following adaptation to face sex, race, and emotion (Webster, Kaping, Mizokami, & Duhamel, 2004). These face aftereffects conform to the idea of norm-based encoding, where stimuli are encoded as a deviation from their psychological norm (Rhodes, Jeffery, Watson, Clifford, & Nakayama, 2003; Rhodes & Leopold, 2009; Valentine, 1991; Valentine & Bruce, 1986). Adaptation results in a temporary shift

* Corresponding author. Tel.: +1 812 855 1554; fax: +1 812 855 4691.
E-mail address: lblaha@indiana.edu (L.M. Blaha).

0028-3932/$ – see front matter © 2010 Elsevier Ltd. All rights reserved.
doi:10.1016/j.neuropsychologia.2010.08.016

of the norm along the adapting dimension, which then influences the subsequent perceptual judgments relying on that same dimension.

Implicit in the norm-based encoding model and similar approaches is the idea that faces are processed along a number of dimensions or labeled lines that work in opposition to code a stimulus. Researchers recently identified that the neural mechanism supporting norm-based encoding is the opponent coding of separate pools of neurons (Robbins, McKone, & Edwards, 2007; Susilo, McKone, & Edwards, 2010). In opponent coding, the endpoints of a feature dimension are coded by separate pools of neurons, and the response of the system is given by the relative activity of the different pools. For a given feature dimension, the norm is the neutral point where the neuron pools are activated equally. This is related to the idea of a visual channel (Graham, 1989) in that the face figural aftereffect is similar to other types of lower level adaptation aftereffects that can lead to the desensitization of the neurons selective for the dimensions of the adapting stimulus (Carandini & Ferster, 1997; Dragoi, Sharma, & Sur, 2000; Movshon & Lennie, 1979; Petersen, Baker, & Allman, 1985). However, several authors have argued that the face aftereffects cannot be explained as a combination of adaptation effects to lower level features such as individual face parts or spatial frequencies (Fang & He, 2005; Köhler & Wallach, 1944; Leopold et al., 2001; Webster et al., 2004; Webster & MacLin, 1999; Yamashita, Hardy, De Valois, & Webster, 2005; Zhao & Chubb, 2001). This suggests that face adaptation might occur at a higher stage of visual processing in groups of neurons with more complex and larger receptive fields (Kovács, Cziraki, Vidnyanszky, Schweinberger, & Greenlee, 2008; Kovács et al., 2006; Kovács, Zimmer, Harza, & Vidnyanszky, 2007; Zhao & Chubb, 2001).

The goal of our current study was to identify the electrophysiological correlates reflecting the figural aftereffects of face adaptation. In a preliminary experiment using distorted (expanded and compressed) face stimuli we first located an event-related potential (ERP) correlate, the P250, that demonstrated systematic modulation to changes in facial distortion. In a second experiment, we manipulated the perceived distortion of the face through an initial adaptation condition and demonstrated how the ERP correlate was affected by both adaptation and distortion. By comparing the ERP correlate of figural aftereffects to other ERP components known to be involved in the face processing stream, we can make inferences about the relative level at which the adapted features and dimensions are involved in face processing. Electrophysiological data have several advantages over behavioral testing, in that they do not require a behavioral response that can be affected by subjective biases about what constitutes a 'normal' stimulus, and they provide time-course information that illustrates the development of adaptation effects in the milliseconds following stimulus onset.

Several human electrophysiology studies of face adaptation have demonstrated that the N170 peak amplitude is decreased following an adapting stimulus relative to control conditions, including both non-adaptation conditions (Kovács et al., 2006; Schweinberger, Kloth, & Jenkins, 2007) and noise image adaptation (Kovács, Zimmer, Harza, Antal, & Vidnyanszky, 2005; Kovács et al., 2007). However, N170 peak suppression is not unique to the adaptation of faces, as it occurs for other images such as hands (Kovács et al., 2006), nor does it differentiate between different adaptation conditions (Schweinberger et al., 2007). The magnitude of the N170 adaptation effects may also depend on the control condition employed, such as hands, faces or $1/f$ visual noise. Thus, the N170 peak suppression may be a general pattern reflecting the presence of an adapting object image, but it may not be as sensitive to manipulations of the adapting stimulus.

These studies of face adaptation generally found that adaptation decreased the N170. However, to directly link the neural correlate to adaptation, an ERP component should show opposite signatures depending on whether the face is being adapted either toward or away from normality. Within the literature no ERP components have yet been identified that correspond to a distorted stimulus appearing more normal as a result of adaptation. Such a finding would identify an EEG/ERP correlate of adaptation reflecting the nature *and direction* of the adaptation rather than the mere presence of an adapting stimulus.

Additionally, the timing of an ERP adaptation component can locate these face mechanisms within the visual stream. If such a component were identified, it might reside in components after the N170. For example, Schweinberger et al.'s (2007) study of gaze adaptation noted that differences between left-gaze and right-gaze adaptation EEG responses were only evident starting at 200 ms after onset of the post-adaptation test stimulus over the right posterior scalp regions. The idea that ERP correlates modulated by adaptation may occur after the N170 is consistent with the suggestion that figural aftereffects occur at later visual processing stages.

Notably, with respect to distorted faces, Halit, de Haan, and Johnson (2000) identified the P2 component, a positive-going waveform occurring 188–300 ms post stimulus onset, as the ERP component modulated by the stretching of a face image. The P2 amplitude was greatest for the normal, unstretched face and exhibited a reduction for both 20% and 30% stretched faces, while the N170 amplitude was not affected by stretching the faces. However, stretching of internal face features within an intact facial surround only represents half of the face distortion dimension along which figural adaptation aftereffects occur; compression of internal face features is the opposite half (Rhodes et al., 2003; Webster & MacLin, 1999). The ERP correlates of face compression remain undefined, since Halit et al. (2000) only examined stretched faces. However, if compression-expansion define a single distortion dimension of face processing, it is likely that the P2 will reflect sensitivity to compression as well as expansion.

To address how distortion, particularly compression, might by itself affect the ERP waveform, we created a continuum of distorted faces, where compressed faces represent the negative side and expanded faces represent the positive side of the distortion continuum, as depicted in Fig. 1. No changes were made to the normal face, which remained in the middle of the distortion continuum. Experiment 1 collected behavioral and neural responses to this continuum of distorted faces to establish the ERP correlate of both compression and expansion distortion. Then, in Experiment 2 we examined the effects of adaptation to illustrate that the ERP correlate of distortion may represent a neural correlate of figural aftereffects.

1. Experiment 1

Our goal in Experiment 1 was to establish the neural correlates of face distortion using a continuum of distortions ranging from compressed to expanded faces. This is a partial replication of prior research that demonstrated a reduction in the amplitude of the ERP response to expanded faces in the P250 component, but the prior work did not include compressed faces (Halit et al., 2000). We asked whether compressed faces would show an enhancement of the ERP activity, or, like expansion, show reduced amplitude to the compressed faces. Although it is possible that compressed faces might increase P250 amplitude, we predict that, like face expansion distortions, the P250 will show a decreased amplitude to compressed faces relative to the undistorted face, thereby reflecting a single ERP component modulated by both types of face distortion.

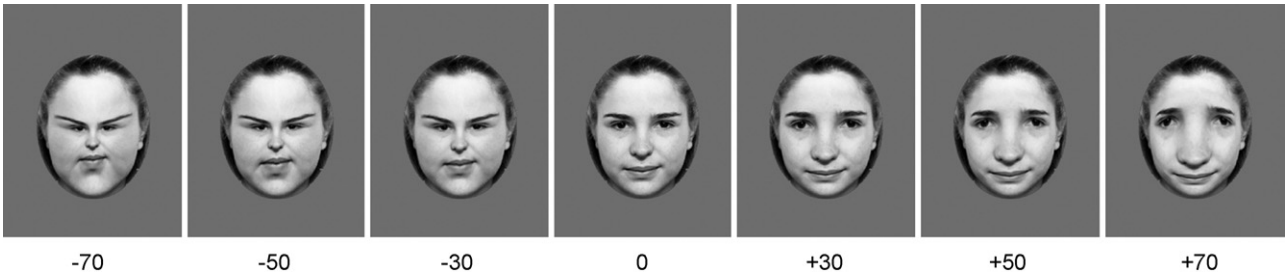

Fig. 1. The range of face distortions for a single face image spanning from highly compressed (−70 face) to highly expanded (+70). The 0 face is undistorted. A larger number in either the positive or negative direction represents greater distortion.

1.1. Method

1.1.1. Participants

Twelve right-handed naïve volunteers from the Indiana University community between the ages of 18 and 35 (7 female, 5 male) participated in this study, in accordance with the standards of the Indiana University Institutional Review Board. Eleven participants were right-handed, and one was left-handed. All participants had normal or corrected-to-normal vision.

1.1.2. Stimuli

The normal, undistorted face stimuli consisted of ten different upright grayscale female faces. A distortion continuum was created for each face by generating seven different distortions ranging from compressed to expanded. The distortions were generated using the Photoshop function Pinch, and Fig. 1 provides an example of one continuum. There were three levels of distortion in both the compressed and expanded sequences, with an undistorted face serving as the normal face. Expanded faces are here represented by positive numbers (+30, +50, +70) with larger numbers signifying a greater amount of distortion according to the value used in Photoshop. Compressed faces are represented with negative numbers (−30, −50, −70) with more negative numbers signifying a greater amount of distortion. Since a normal face was undistorted, it is numerically represented with a 0. The combination of these 7 levels of distortion performed on 10 faces yielded a total of seventy different face images used throughout Experiment 1.

The faces' luminance values varied from 2.7 to 93.0 candelas/m^2. The background's luminance value was 33.8 candelas/m^2. The faces had a height of 15.6 cm and a width of 12.1 cm. At a viewing distance of 46 in (112 cm), the faces subtended a visual angle of 8° vertical and 5.96° horizontal.

1.1.3. Apparatus

The EEG was sampled at 32 channels at 1000 Hz and downsampled to 250 Hz. It was amplified by a factor of 20,000 using Sensorium amps and low-pass filtered below 50 Hz. All channels had below 10-kΩ impedance (usually below 5-kΩ), and recording was done inside a Faraday cage. The nose electrode served as the reference for all electrodes except the horizontal and vertical eye channels, each of which had their own reference electrodes.

Images were shown on a gamma-calibrated 21-in. (53.34 cm) Mitsubishi color monitor model THZ8155KL running at 120 Hz.

1.1.4. Procedure

The experiment consisted of 840 trials with seven different conditions representing the seven levels of distortion per each of ten faces. An equal number of trials (n = 120) were presented per distortion condition. Each trial showed a single face centered on the screen for 500 ms, although there was no specified fixation point. The blank screen interstimulus interval (ISI) was uniformly distributed between 325 and 517 ms. EEG was recorded from 100 ms prior to stimulus onset to 500 ms post stimulus onset.

Participants were instructed to rate each face as either compressed, normal, or expanded via key press on a number pad. The participants were instructed to press the number 1, 2, or 3 if they saw a compressed, normal, or expanded face, respectively. Participants were able to freely view the images, although they were instructed to limit both their eye and body movements while a stimulus was on the screen.

1.1.5. ERP component selection and analysis

The peak amplitude and latency for each ERP component of interest, P100, N170 and P250, were selected by an algorithm in MATLAB within the following pre-specified time windows: P100 peak values were selected as the maximum amplitude in the time window 80–120 ms post stimulus onset. N170 peak values were selected as the minimum amplitude in the window 125–180 ms post stimulus onset. P250 peak values were selected as the maximum amplitude in the window 184–260 ms post stimulus onset.

We primarily examined the ERP components identified at the PO8 and PO7 channels, right and left posterior–temporal scalp electrodes in the 10–10 system, for the neural correlates of face distortion because these channels have repeatedly shown clear waveforms when processing complex objects such as faces (e.g., Bentin & Deouell, 2000) and are the electrode locations most similar to those exhibiting the strongest modulation by face distortion in previous research (Halit et al., 2000).

The EEGLab toolbox (Delorme & Makeig, 2004) was employed for EEG data analysis. Independent component analysis (ICA) was used to identify artifacts such as eye-blinks, eye movements, and muscle activity. The eye-related artifacts were identified via their topographical representation on the scalp through blink and eye-movement calibration trials at the beginning of the experiment. High-frequency amplitude spectrum and topographical representation was used to identify independent components relating to muscle artifacts. Between three to eight independent components were removed for each participant during the ICA pre-processing. These artifacts were subtracted from the raw EEG data prior ERP analyses.

1.2. Results

1.2.1. Behavioral results

In order to more directly compare the behavioral ratings to the ERP data, we transformed the raw behavioral ratings into perceived deviation from normality ratings by first subtracting each subject's raw normality ratings from his/her rating of the 0 distortion face. Second, we took the absolute value of the deviation scores. In this way, the perceived deviations from normality were centered around a value of 0 for the undistorted face image. Fig. 2 shows the average deviation from normality ratings for all distortion conditions. Fig. 2 illustrates that perceived deviation from normality increased as physical distortion of the image increased.

We analyzed the deviation from normality ratings with a one-way repeated measures analysis of variance (ANOVA) with the

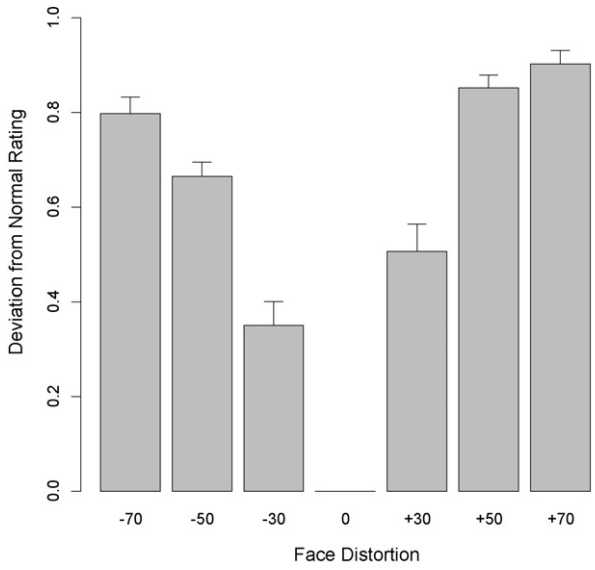

Fig. 2. Average deviation from normality ratings. Normality ratings were centered such that an undistorted face had a mean deviation rating of 0. A larger deviation score indicates a higher degree of deviation from what the participants rated as normal. This pattern mirrors the modulation of the P250 component from distortion found in Figs. 3 and 4. Error bars indicate +1 standard error of the mean.

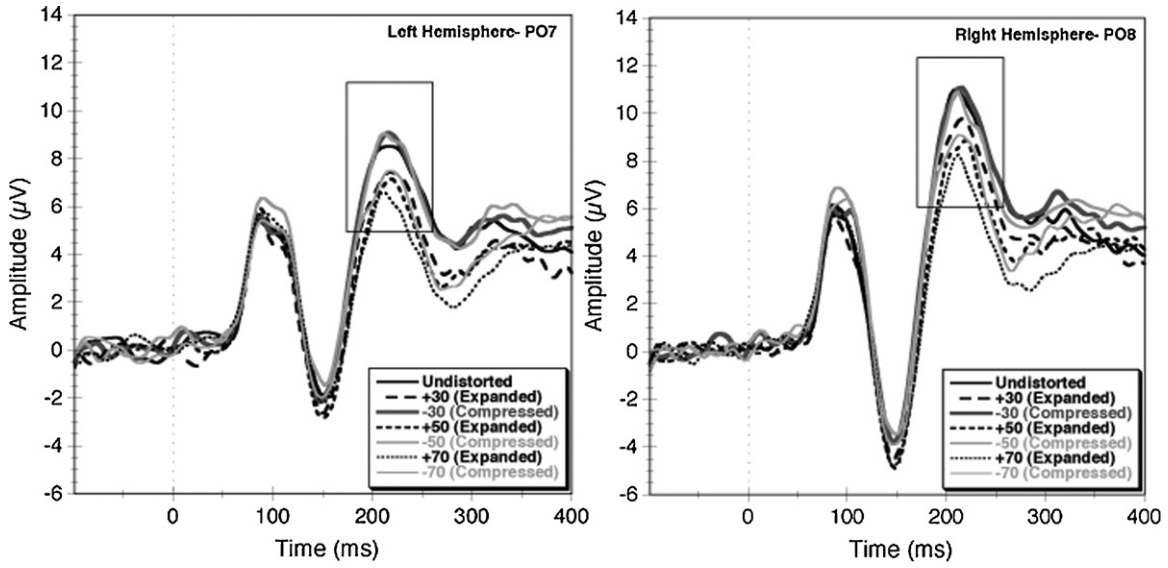

Fig. 3. Grand average ERP results from Experiment 1 for the PO7 and PO8 electrodes. The P250, the outlined positive component around 220 ms, is systematically modulated by distortion. The pattern demonstrates that faces perceived to be more normal have larger P250 amplitudes.

within-subjects factor distortion (7 levels). There was a significant effect of distortion on perceived deviation from normality ($F(6,66) = 114.23$, $p < .001$).

Fig. 2 further indicates that deviation from normality ratings were not identical for the physically equal levels of face compression and expansion. Rather the expanded faces were perceived as deviating more from the normal, undistorted face than the compressed faces of equal physical manipulation. Post hoc paired *t*-tests showed that the +30 face had a higher average deviation from normality rating ($M_{+30} = 0.51$, $SD_{+30} = 0.19$) than the −30 face ($M_{-30} = 0.35$, $SD_{-30} = 0.17$; $t(11) = 3.32$, Bonferroni corrected $p = .02$), and the +50 face had a higher deviation from normality rating ($M_{+50} = 0.85$, $SD_{+50} = 0.09$) than the −50 face ($M_{-50} = 0.66$, $SD_{-50} = 0.10$; $t(11) = 6.58$, Bonferroni corrected $p < .001$). The +70 face showed a marginally significantly larger deviation from normality ($M_{+70} = 0.90$, $SD_{+70} = 0.09$) than the −70 face ($M_{-70} = 0.80$, $SD_{-70} = 0.11$; $t(11) = 2.75$, Bonferroni corrected $p = .06$).

1.2.2. Electrophysiological results

The grand average ERPs for all face distortion conditions are plotted in Fig. 3, and the mean peak amplitudes for the N170 and P250 ERP components are plotted in Fig. 4. Both peak amplitude and peak latency for each of the P100, N170 and P250 were analyzed with two-way repeated measures ANOVAs with the within-subjects factors of distortion (7 levels: −70, −50, −30, 0, +30, +50, +70) and hemisphere (2 levels: left (PO7), right (PO8)). ANOVA results are summarized in Table 1.

1.2.2.1. P100. There were no differences in either P100 peak amplitude or latency across distortion condition, nor were there P100 differences across hemispheres.

1.2.2.2. N170. There was a significant main effect of distortion on N170 peak amplitude ($F(6,60) = 2.44$, $p = .04$). Looking at the top row of Fig. 4, we see that the mean peak amplitude of the N170 ERP component exhibits some increases (more negative peaks) for the expanded face distortion conditions compared with the 0 distortion condition. Compressed face conditions exhibited N170 peak amplitudes approximately equal to or less than (less negative peaks) the undistorted face conditions.

Post hoc paired two-tailed *t*-tests were performed to compare each distorted face to the undistorted face, to determine the pattern of deviations from the amplitude exhibited by the undistorted face. Considering first the compressed faces, Fig. 4 indicates that compressed faces may show some reduction in peak amplitude relative to the undistorted face condition. There were no differences between the peak amplitudes to the undistorted face condition ($M_0 = -4.74$, $SD_0 = 5.42$) and any of the compressed face conditions (−30 face: $M_{-30} = -4.62$, $SD_{-30} = 6.14$; $t(11) = 0.29$, $p = .78$; −50 face: $M_{-50} = -4.20$, $SD_{-50} = 5.64$, $t(11) = 1.23$, $p = .24$; −70 face: $M_{-70} = -4.75$, $SD_{-70} = 5.20$, $t(11) = 0.03$, $p = .97$).

In Fig. 4, expanded face conditions appear to show some increases in peak amplitude relative to the undistorted face condition. The +50 expanded face ($M_{+50} = -5.67$, $SD_{+50} = 5.43$) exhibited a significantly larger (more negative) amplitude than the undistorted face ($t(11) = 2.29$, $p = .04$). There were no differences between the undistorted face and both the +30 expanded face condition ($M_{+30} = -5.21$, $SD_{+30} = 5.07$; $t(11) = 1.28$, $p = .23$) and the +70 expanded face condition ($M_{+70} = -5.26$, $SD_{+70} = 5.15$; $t(11) = 1.37$, $p = .20$). Thus, almost all distorted face conditions exhibited mean peak amplitudes approximately equal to the peak amplitude in the undistorted face condition.

There were no differences in N170 latency across distortion condition or hemisphere.

1.2.2.3. P250. For P250 peak amplitude, there was a significant main effect of distortion ($F(6,60) = 6.47$, $p < .001$). Looking at the bottom row of Fig. 4, we see that as the magnitude of distortion increased from 0, the mean peak amplitude of the P250 ERP component either remained equal to or decreased from the peak amplitude in the 0 distortion condition. P250 peak amplitude to expanded faces strictly decreased as the magnitude of distortion increases, while the P250 response to compressed faces only exhibited a decrease in peak amplitude to the −70 compressed face.

Post hoc paired two-tailed *t*-tests were used to compare the mean peak amplitudes of neighbors along the distortion continuum. Considering first the compressed distorted faces, the −70 compressed face ($M_{-70} = 9.42$, $SD_{-70} = 4.25$) had a significantly lower peak amplitude than the −50 compressed face ($M_{-50} = 10.86$, $SD_{-50} = 4.76$; $t(11) = 3.50$, $p = .005$). But no differences were observed between the mean peak amplitude of the undistorted face ($M_0 = 10.74$, $SD_0 = 4.62$) and the −30 face ($M_{-30} = 11.10$, $SD_{-30} = 5.87$; $t(11) = 0.67$, $p = .52$), or between the −30 and −50 faces ($t(11) = 0.56$, $p = .59$).

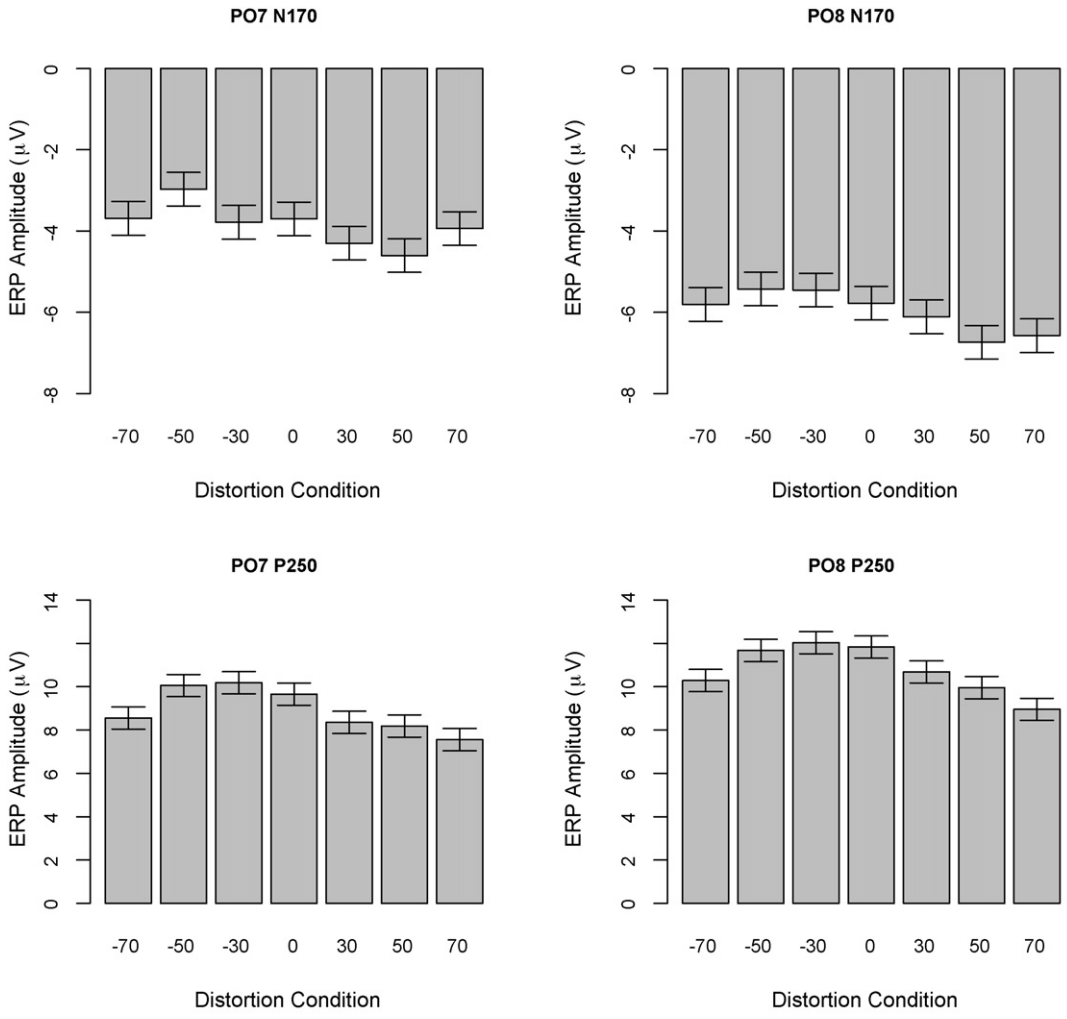

Fig. 4. Mean ERP peak amplitude across face distortion conditions for the N170 and P250 components in Experiment 1. Only the P250 reflects systematic differences observed across distortion levels. The P250 peak amplitudes mirror the ordering of deviation from normality ratings (Fig. 2). Error bars show ±1 standard error.

For the expanded faces, the +30 expanded face (M_{+30} = 9.52, SD_{+30} = 4.37) exhibited a significantly smaller amplitude than the undistorted face ($t(11)$ = 2.69, p = .02). There was a trend for the +70 expanded face (M_{+70} = 8.25, SD_{+70} = 5.08) to exhibit a smaller amplitude than the +50 expanded face (M_{+50} = 9.06, SD_{+50} = 4.52; $t(11)$ = 1.88, p = .09). No difference was observed between the +30 and +50 expanded faces ($t(11)$ = 1.06, p = .31). For expanded faces, then, P250 peak amplitude decreased as the amount of distortion increased. Thus, P250 peak amplitude generally decreases as faces become more distorted and less normal regardless of the type of distortion, although a larger degree of physical compression is needed to produce a decrease in amplitude similar to the decrease observed for all expanded faces. This pattern of peak amplitude reduction mimicks the u-shaped pattern observed in the deviation from perceived normality ratings behavioral data.

P250 peak latency exhibited no differences across distortion levels or hemisphere.

1.2.3. Correlations

To examine the potential relationship between the deviation from normality behavioral measure and the ERP peak amplitudes, we estimated the correlation coefficients for each of the ERP components (P100, N170, P250) at both the PO7 and PO8 electrode locations. The correlation coefficients are summarized in Table 2,

Table 1
Experiment 1 ANOVA results.

	df	Peak amplitude			Peak latency		
		P100 *F*	N170 *F*	P250 *F*	P100 *F*	N170 *F*	P250 *F*
Electrode location (L)	1	<1.0	<1.0	1.57	<1.0	<1.0	1.21
S within-group error	10	(151.87)	(302.43)	(210.92)	(1937.60)	(953.30)	(1110.90)
Test distortion (T)	6	1.09	2.44**	6.47***	<1.0	1.09	<1.0
T × L	6	<1.0	<1.0	<1.0	1.05	1.11	1.00
T × S error	60	(1.79)	(1.03)	(1.58)	(32.58)	(17.12)	(71.40)

Note: Values in parenthesis represent mean square errors. S = subjects.
** $p < .05$.
*** $p < .01$.

Table 2
Correlation coefficient estimates for Experiment 1.

Subject	P100		N170		P250	
	PO7	PO8	PO7	PO8	PO7	PO8
1	.14	.48	−.27	−.43	−.57	−.55
2	−.30	.37	.68*	.66	.03	.29
3	−.22	−.61	.61	−.38	−.14	−.76**
4	−.14	.05	.02	.22	−.51	−.54
5	.51	.75*	.38	−.16	−.13	−.45
6	−.25	−.07	−.66	−.51	−.75**	−.49
7	−.72*	−.22	−.009	.25	−.69*	−.50
8	.06	−.26	−.37	−.51	−.81**	−.92***
9	.64	−.05	.27	.13	.06	−.16
10	.23	.08	−.14	−.25	.001	−.25
11	.06	.33	−.35	−.23	−.57	−.07
12	−.17	−.36	−.36	−.66	−.48	−.94***
Overall	**.13**	**.06**	**−.19**	**−.54**	**−.65**	**−.79****

* $p < .10$ in a two-tailed test.
** $p < .05$ in a two-tailed test.
*** $p < .01$ in a two-tailed test.

which includes both the estimates for each subject, as well as the overall correlation coefficients. The overall correlation coefficients were estimated by finding the correlations between the grand average deviation from normality rating scores and the grand average ERP component peak amplitudes.

From Table 2, we can see that overall there is no correlation between both the P100 peak amplitude and the deviation from normality scores and the N170 peak amplitude at the deviation from normality scores. There are strong overall correlations between the perceived amount of deviation from normality as shown in Fig. 2 and the P250 peak amplitude at the both the PO8 channel ($r = -.79$, $t(5) = -2.85$, $p = .04$) and P07 electrodes ($r = -.65$, $t(5) = -1.93$, $p = .11$). In addition, eleven out of the twelve subjects have negative correlations, and both overall correlations are negative, reflecting the fact that across the distortion levels, as there is an increase in people's perceived deviation from normality, the corresponding P250 peak amplitude is decreasing. Thus we can conclude that the P250 peak amplitude is modulated by the perceived distortion of faces.

1.3. Discussion

The results of Experiment 1 provide an important extension of the results of Halit et al. (2000) by demonstrating that the P250, a positive-going waveform immediately following the N170, is systematically modulated by both expansion and compression face distortions. We demonstrated that as the amount of perceived distortion increases, the peak amplitude of the P250 component decreases, regardless of whether the distortion was caused by expansion or compression of the face features. However, the results indicate that a larger degree of face compression than expansion is needed to produce a reduction in the P250 amplitude. This electrophysiological pattern has a strong association with the u-shaped perceived deviation from normality pattern found in the behavioral results. Additionally, the results that a larger degree of compression is needed to produce a P250 amplitude reduction is consistent with the behavioral results in that ratings of compressed faces exhibited smaller deviation from normality scores than the ratings of expanded faces of equal magnitude.

The perceived distortion of faces showed little systematic modulation of the P100 ERP component, but did exhibit some limited modulation of the N170 component with only one expanded face condition leading to a strong difference in peak amplitudes. This pattern does not reflect the perceived distortion measured in our behavioral ratings. It remains unclear if the observed modulation of the N170 reflects physical differences in the faces due to the opposite manipulations of compressing the features toward the center of the faces and expanding the features toward the outer edges of the faces.

Thus, the results of Experiment 1 identified a single ERP correlate sensitive to a face distortion continuum and reflecting the participants' perceived distortions in the images. For this correlate, the P250 amplitude, we confirmed that any type of face distortion results in a decrease in ERP amplitude, although the size of the ERP effect is modulated somewhat by the amount of physical distortion in the face images. Therefore, the P250 amplitude may reflect a single dimension of face distortion representation within a norm-based encoding scheme. The results of Experiment 1 further suggest that the P250 ERP component may reflect changes in perceived distortion following adaptation, termed figural aftereffects. We will use this neural correlate in Experiment 2 to address how adaptation affects the neural substrates of distortion perception.

2. Experiment 2

The results of Experiment 1 identified a metric relating the amount of distortion, regardless of the direction of distortion, and ratings of perceived distortion, to changes in the P250 peak amplitude. Faces that were perceived as more normal produced greater P250 amplitudes. Experiment 2 uses this metric to address whether adaptation affects the same neural sources that are sensitive to perceptual distortions. We used an initial adaptation condition to perceptually distort the subsequent test faces either toward or away from normality. We analyzed the effect of adaptation on these distorted test faces by comparing their P250 ERP component amplitudes across adaptation conditions, to see whether the test faces showed a perceptual change in the hypothesized direction.

We predict that distorted test faces will exhibit higher P250 peak amplitudes in adaptation conditions that result in test faces being perceived as more normal. Specifically, adapting to an expanded face will result in a less expanded face appear more normal and a compressed face appear less normal (Webster & MacLin, 1999); therefore, in the expanded face adaptation condition, a less expanded face should exhibit a larger P250 peak amplitude. The opposite result is predicted for the compressed face adaptation condition: a less compressed face is perceived as more normal and should exhibit a larger P250 peak amplitude than an expanded face.

Central to our approach is a design that varies the adaptation state of the subject while holding constant the distortion level of the face. This allows us to isolate the effects of adaptation for both expanded and compressed test faces.

2.1. Method

2.1.1. Participants

Twelve Indiana University students between the ages of 18 and 28 (4 female, 8 male) participated voluntarily in this study, in accordance with the standards of the Indiana University Institutional Review Board. Three participants (AB, DW, LB) were among the authors, so were knowledgeable of the purpose and details of the experiment. Eleven participants reported right-hand dominance, and one was left-handed. All participants had normal or corrected-to-normal vision. No Experiment 2 volunteers were participants in Experiment 1.

2.1.2. Stimuli

The stimuli consisted of nine different distortions of a single grayscale female face. These distortions ranged along a continuum from compressed to expanded, and were created using the Photoshop function Pinch, as in Experiment 1. For Experiment 2, the distortion levels for compressed and expanded faces in decreasing amounts of distortion were −50, −40, −30, −20 and +50, +40, +30, +20, respectively. The normal face was numerically represented with a 0. The ±20, ±30, and ±40 distorted faces are depicted in the inset of Fig. 5, and the 0 and ±50 faces are shown as the adapting faces.

The face images' sizes, visual angles, and luminance values were identical to those in Experiment 1.

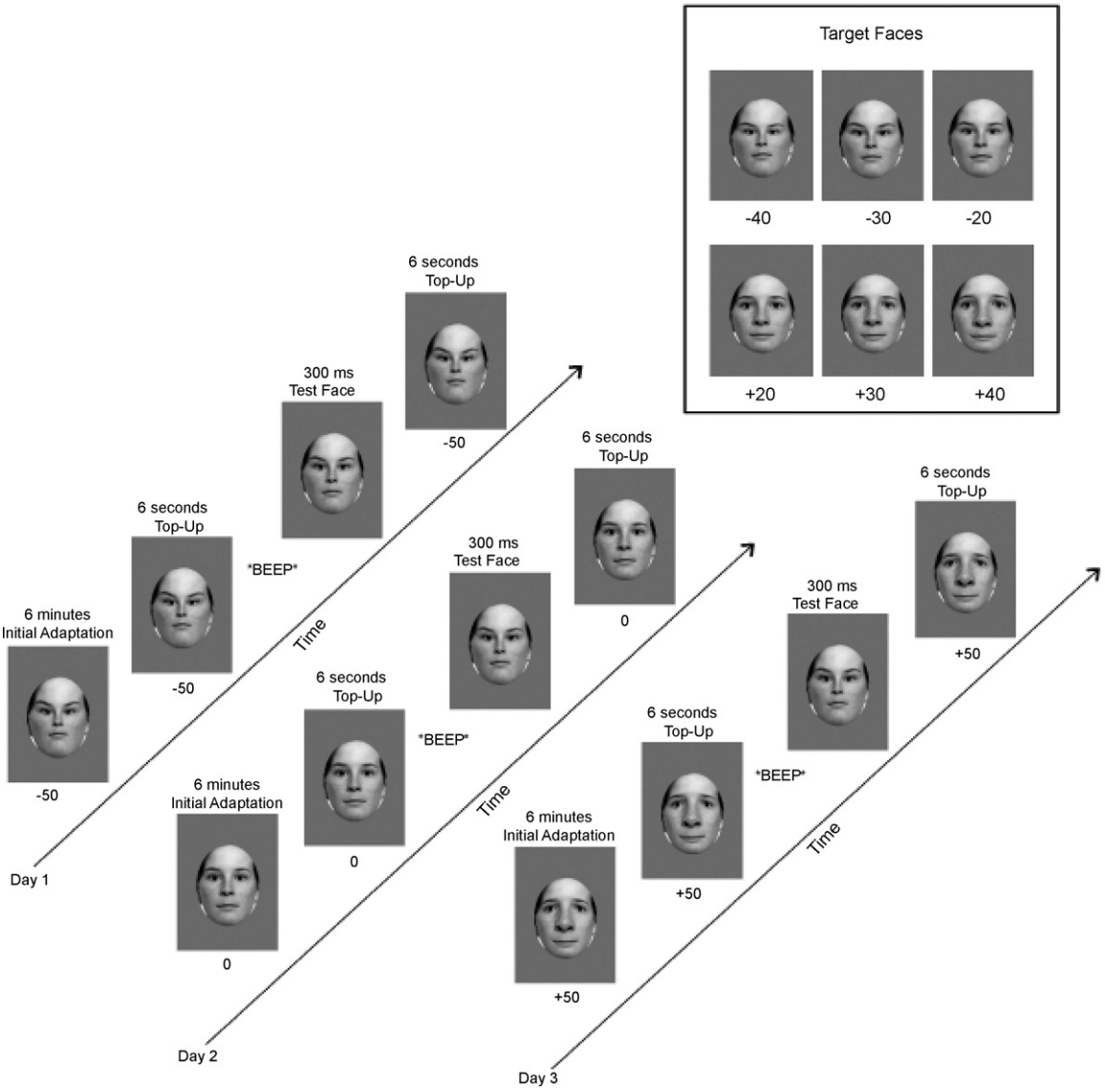

Fig. 5. Diagram of Experiment 2. A different adaptation condition (−50, 0, +50) was used on each day of training, with the order counterbalanced across subjects. The upper right inset box shows the set of test faces, only one of which was shown on each trial.

2.1.3. Apparatus

All testing apparatus were the same as Experiment 1.

2.1.4. Procedure

A schematic diagram of Experiment 2 is depicted in Fig. 5. Experiment 2 consisted of three testing days, with 320 trials per day. The 320 trials were divided among six test face conditions: −30 (n = 120 trials), +30 (n = 120), −20 (n = 20), +20 (n = 20), −40 (n = 20), and +40 (n = 20). While the ±30 test faces are our primary test conditions of interest, the inclusion of the ±20 and ±40 faces served to encourage participants to rely on their individual percepts rather than use an algorithmic approach to the normality ratings (e.g., "I always give compressed faces a 5 rating and expanded faces a 3 rating.").

Participants were tested with a different adaptation condition on each testing day. Three adaptation conditions were used: highly compressed face (−50), undistorted face (0), and highly expanded face (+50). The order of adaptation conditions was counterbalanced across subjects. Adaptation testing began with an initial six-minute adaptation phase to the given condition for that day. During this time, the participants were told to fixate on the adapting face, and an auditory beep signaled the passing of each minute. No responses were made during the initial adaptation period.

After the initial six-minute adaptation period, each trial was preceded by a 6 s top-up presentation of the adapting face. This served to refresh the adaptation effect. After the top-up, there was a blank screen of variable delay, uniformly distributed between 324 and 516 ms together with an auditory beep signaling the participants that the target face was about to be presented. Target faces were presented centrally for 300 ms, followed by a blank screen until the participants responded. Responses were immediately followed by the next 6 s top-up face, with no inter-trial delay. EEG was recorded at 100 ms prior to stimulus onset to 500 ms post stimulus onset.

In recognition of the fact that the electrophysiological correlate reflects the *amount* of distortion regardless of the *direction* of the distortion, we also altered our behavioral response to avoid having to transform it later. Participants were instructed to rate the face on a normality scale from 1 to 7 via a number pad key press, where 1 was a normal, undistorted face and 7 was a highly distorted, non-normal face. Participants were able to freely view the images, although they were instructed to limit both their eye and body movements while a stimulus was on the screen.

2.1.5. ERP component selection and analysis

ERP component peak amplitudes and latencies were selected using the same MATLAB algorithm described in Experiment 1. The following time windows were used for selecting the peak amplitudes and latencies from the PO7 and PO8 electrodes: P100, 80–120 ms; N170, 125–180 ms; N250, 184–260 ms. EEG data were analyzed with the EEGLab toolbox (Delorme & Makeig, 2004), and muscle artifacts were removed by ICA, as described in Experiment 1.

2.1.6. Statistical analyses

Unless otherwise stated, all statistical analyses are limited to the data from ±30 test faces. For the electrophysiological results, we analyzed grand average ERP data from the PO8 and PO7 electrodes, where the strongest metric reflecting face distortion was identified in Experiment 1.

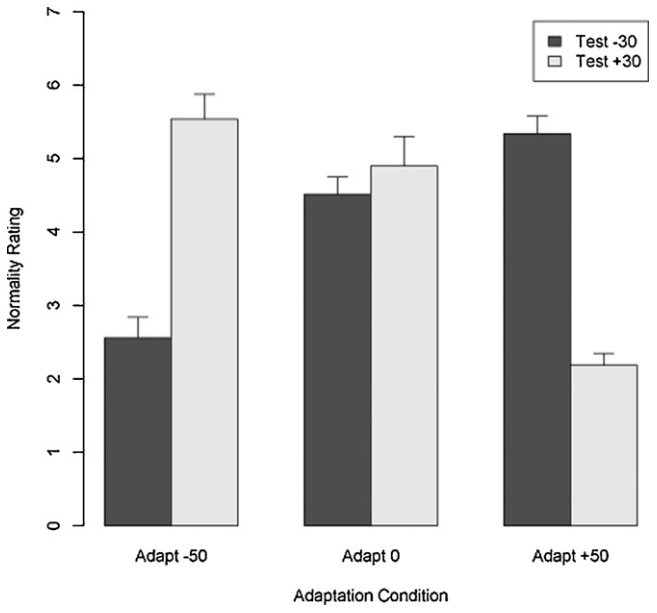

Fig. 6. Average normality ratings for Experiment 2. The normality scale ranged from 1 (undistorted, normal face) to 7 (highly distorted, non-normal face); thus a higher rating indicates that a face was perceived as less normal. The normality ratings reflect a crossover interaction between the −50 and +50 adaptation conditions. Error bars show +1 standard error.

2.2. Results

2.2.1. Behavioral results

The mean normality ratings for both the ±30 test faces in all three adaptation conditions are shown in Fig. 6. The mean normality ratings support the behavioral predictions for figural aftereffects. In the +50 adaptation condition (adapt to an expanded face), the +30 test was rated as more normal ($M_{+30} = 2.2$, $SD_{+30} = 0.6$) than the −30 test face ($M_{-30} = 5.3$, $SD_{-30} = 0.8$). In the −50 adaptation condition (adapt to a compressed face), the opposite pattern was observed: the +30 test face was rated as less normal ($M_{+30} = 5.5$, $SD_{+30} = 1.2$) than the −30 test face ($M_{-30} = 2.6$, $SD_{-30} = 1.0$).

Rating scores were analyzed with a two-way repeated measures ANOVA with the within-subjects factors of adaptation (three levels: 0, −50, +50) and test distortion (two-levels: −30, +30). There was a significant main effect of adaptation condition ($F(2,22) = 7.42$, $p = .003$) and a signification adaptation by test distortion interaction ($F(2,22) = 48.11$, $p < .001$). There was no effect of test distortion ($F(1,11) < 1$, $p = .77$). Post hoc pairwise t-tests confirm that the +30 test was rated significantly lower than the −30 test faces in the +50 adaptation condition ($t(11) = 14.81$, Bonferroni corrected $p < .001$), and the +30 test was rated significantly higher than the −30 test face in the −50 adaptation condition ($t(11) = 5.75$, Bonferroni corrected $p < .001$). There was no difference between the +30 and −30 test faces in the 0 adaptation condition ($t(11) = 0.70$, Bonferroni corrected $p = 1.0$).

These behavioral data indicate that the adaptation conditions produce strong perceptual effects that alter the rated normality of the test faces in different ways, sometimes making a face appear more normal and sometimes making it appear more distorted.

2.2.2. Electrophysiological results

Mean peak amplitude results for all ERP components of interest are shown in Fig. 7. For each ERP component, P100, N170 and P250, we conducted two three-way repeated measures ANOVAs with the within-subject factors of adaptation (3 levels: 0, −50, +50), test distortion (2 levels: −30, +30) and electrode location (2 levels: PO7, PO8). One ANOVA for each component was conducted on the dependent measure peak amplitude of the ERP waveform, and the second ANOVA for each component was conducted on the dependent measure latency of the component peak.

ANOVA results are summarized in Table 3.

2.2.2.1. P100. For P100 peak amplitude (Fig. 7, top row), there was a marginally significant main effect of electrode location. Average peak amplitude of the PO8 electrode tended to be greater ($M_{PO8} = 12.61$, $SD_{PO8} = 3.51$) than the average peak amplitude of the PO7 electrode ($M_{PO7} = 6.21$, $SD_{PO7} = 7.13$). There were no other significant main effects or interactions on the P100 peak amplitude.

For P100 peak latency, there were no significant main effects or interactions.

2.2.2.2. N170. For the N170 peak amplitude (Fig. 7, middle row), there was a marginally significant main effect of test distortion, reflecting a strong trend that the average N170 peak amplitude was more negative in the +30 test distortion condition ($M_{+30} = -2.51$, $SD_{+30} = 6.02$) than in the −30 test distortion condition ($M_{-30} = -1.95$, $SD_{-30} = 5.43$). There was a marginally significant adaptation by test distortion interaction. There were no other main effects or interactions for N170 peak amplitude.

In the ERP waveforms depicted in Fig. 8, there is evidence that the marginally significant adaptation by test distortion interaction is a crossover interaction, with the +30 test face condition having a more negative amplitude in the Adapt −50 condition, and the −30 test face condition showing a more negative amplitude in the Adapt +50 condition. We further tested the marginally significant adaptation by test distortion interaction with post hoc two-tailed paired t-tests. In the Adapt +50 condition, there was a trend for the −30 test distortion condition to show a more negative peak amplitude ($M_{-30} = -2.24$, $SD_{-30} = 5.10$) than the +30 test distortion condition ($M_{+30} = -1.19$, $SD_{+30} = 5.42$; $t(11) = 2.14$, Bonferroni corrected $p = .17$). The Adapt −50 condition showed the opposite trend, with the −30 test distortion condition showing a less negative peak amplitude ($M_{-30} = -2.07$, $SD_{-30} = 6.34$) than the +30 test distortion condition ($M_{+30} = -3.57$, $SD_{+30} = 6.68$; $t(11) = 1.86$, Bonferroni corrected $p = .27$). There was no difference between the +30 and −30 test distortions in the 0 adaptation condition ($t(11) = 0.75$, Bonferroni corrected $p = 1.0$). Thus, we have some limited evidence for a trend-level crossover interaction between adaptation conditions at the N170 peak amplitude. However, the marginally significant adaptation by test distortion interaction is primarily the result of the difference in peak amplitudes between the +30 and −30 test distortions in the Adapt −50 condition only.

For N170 peak latency, there were no significant main effects or interactions.

2.2.2.3. P250. For the P250 peak amplitude (Fig. 7, bottom row), there was a significant main effect of test distortion ($F(1,10) = 4.85$, $p = .05$), reflecting that average peak amplitude in the −30 test distortion condition ($M_{-30} = 9.77$, $SD_{-30} = 5.74$) was greater than the average peak amplitude in the +30 test distortion condition ($M_{+30} = 9.07$, $SD_{+30} = 6.20$). There was a marginally significant main effect of electrode location, indicating that there was a strong trend for the average PO8 peak amplitude ($M_{PO8} = 12.29$, $SD_{PO8} = 4.57$) to be greater than the average PO7 peak amplitude ($M_{PO7} = 6.54$, $SD_{PO7} = 5.80$). There was no main effect of adaptation.

There was a significant adaptation by test distortion interaction ($F(2,20) = 9.67$, $p = .001$).

Post hoc paired comparisons show that the significant interaction is a crossover interaction at both the PO7 and PO8 electrodes. In the −50 adaptation condition, +30 test faces exhibited significantly smaller peak amplitudes than the −30 test faces (PO7: $t(11) = 3.16$, Bonferroni corrected $p = .05$; PO8 $t(11) = 3.23$, PO8 Bonferroni corrected $p = .05$). In the +50 adaptation condition, +30 test faces

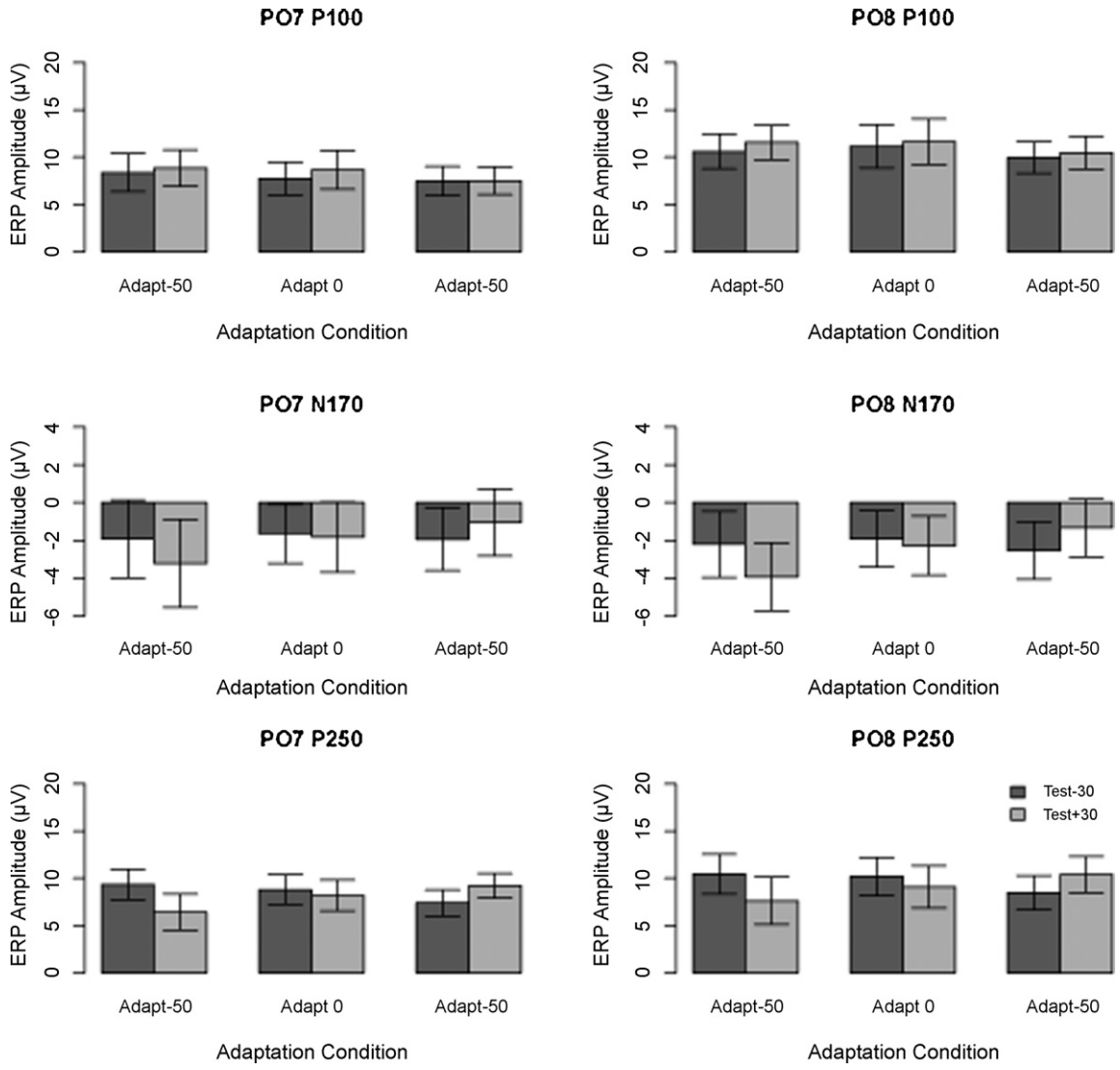

Fig. 7. Mean peak amplitudes for the P100, N170, and P250 ERP components in Experiment 2 across all adaptation conditions. Dark bars show the mean peak amplitude for the −30 test faces, and light bars show the mean peak amplitude for the +30 test faces. Error bars show ±1 standard error.

exhibited significantly larger peak amplitudes than −30 test faces (PO7: $t(11) = 3.10$, Bonferroni corrected $p = .06$; PO8 $t(11) = 3.34$, Bonferroni corrected $p = .04$). There was no difference between the P250 peak amplitude of the +30 and −30 test faces in the 0 adaptation condition (PO7: $t(11) = 1.76$, Bonferroni corrected $p = .64$; PO8: $t(11) = 2.51$, Bonferroni corrected $p = .17$).

This significant crossover interaction for the P250 ERP component is illustrated in the grand average ERP curves in Fig. 8. The

Table 3
Experiment 2 ANOVA results.

	df	Peak amplitude			Peak latency		
		P100 *F*	N170 *F*	P250 *F*	P100 *F*	N170 *F*	P250 *F*
Electrode location (L)	1	3.73*	<1.0	3.99*	<1.0	1.42	3.90*
S within-group error	10	(197.63)	(192.38)	(149.63)	(997.90)	(1186.20)	(920.20)
Adaptation (A)	2	<1.0	1.79	<1.0	<1.0	2.38	<1.0
A × L	2	<1.0	1.20	<1.0	1.20	1.76	1.16
A × S error	20	(7.49)	(10.21)	(11.97)	(102.84)	(59.38)	(259.00)
Test distortion (T)	1	<1.0	3.65*	4.85**	<1.0	<1.0	3.38*
T × L	1	<1.0	<1.0	<1.0	1.49	<1.0	1.27
T × S error	10	(2.71)	(1.54)	(1.85)	(33.64)	(17.29)	(63.16)
A × T	2	<1.0	2.92*	9.67***	<1.0	1.43	1.05
A × T × L	2	<1.0	<1.0	<1.0	<1.0	1.54	<1.0
A × T × S error	20	(1.52)	(2.94)	(3.02)	(69.51)	(35.56)	(57.16)

Note: Values within parentheses are mean square errors. S = subjects.
* $p < .10$.
** $p < .05$.
*** $p < .01$.

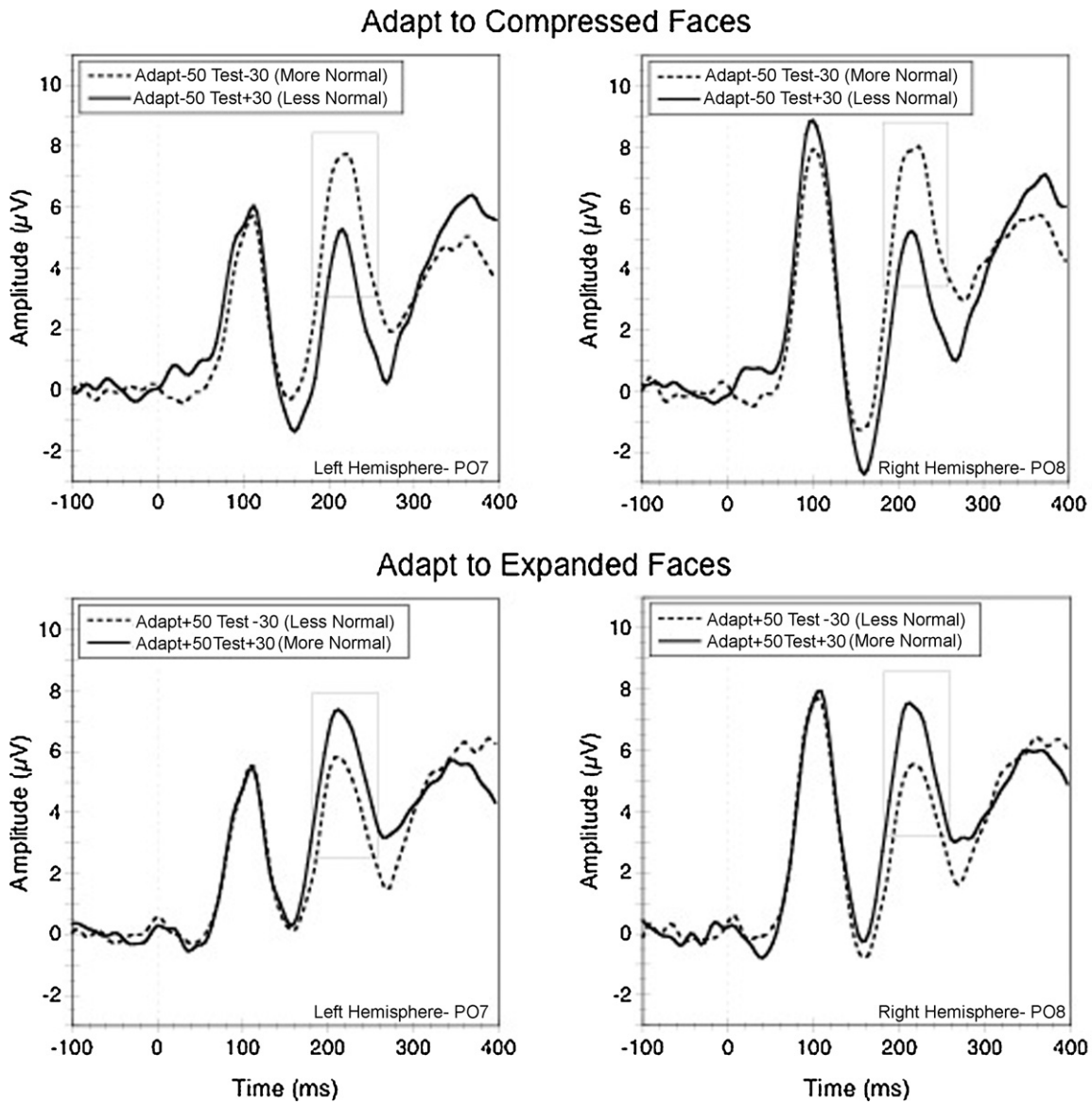

Fig. 8. The grand average ERP results from Experiment 2 with only the −50 (top row) and the +50 adaptation conditions (bottom row) in the P07 and PO8 Channel. The P250, the outlined positive component around 220 ms, illustrates the crossover interaction of distortion with the adapting condition (compressed or expanded).

top row shows the curves for the +30 and −30 test faces in the −50 adaptation condition. Adapting to a compressed face made the −30 (compressed) test face appear more normal and the +30 (expanded) faces appear less normal. Thus, the −30 test face produces a larger P250 peak amplitude than the +30 test face in the top row of Fig. 8. Adapting to an expanded (+50) face produced the opposite result illustrated in the bottom row of Fig. 8: the +30 test face produced a larger P250 peak amplitude than the −30 test face. Thus, adaptation to an expanded face made other expanded faces appear more normal and the compressed faces appear less normal.

For P250 peak latency, there was a marginally significant main effect of test distortion, indicating a strong trend that average peak latency in the −30 test distortion condition (M_{-30} = 219.11, SD_{-30} = 15.54) was later than the average peak latency in the +30 test distortion condition (M_{+30} = 215.67, SD_{+30} = 18.87). There was a marginally significant effect of electrode location, reflecting the strong trend that the average PO8 peak latency was later (M_{PO8} = 224.44, SD_{PO8} = 18.29) than the average PO7 peak latency (M_{PO7} = 210.33, SD_{PO7} = 12.81). There were no other significant main effects or interactions.

The complete spatial extent of the effects of adaptation can be seen in Fig. 9, which shows three time-slices of the modulation of adaptation. To create these difference maps, we subtracted EEG voltages in the +30 distortion condition from the −30 distortion condition and plotted the mean difference at each electrode, with spatial interpolation filling in the space between the electrodes. The color reversal seen in the left and right columns comes from the fact that the +50 and −50 adaptation conditions produce opposite results on the +30 and −30 test faces, leading to the crossover interaction. As can be seen, the adaptation modulation begins to appear in the 170 ms time period, and is more robust (and statistically significant) around 225 ms. Adapting to the normal face tends not to produce strong modulations of perceived distortion, which is evidenced by the lack of color changes in the central column at any timeslice.

2.3. Discussion

Experiment 2 data demonstrated that an adapting stimulus affects both the perceived distortion of a face and the electrophysi-

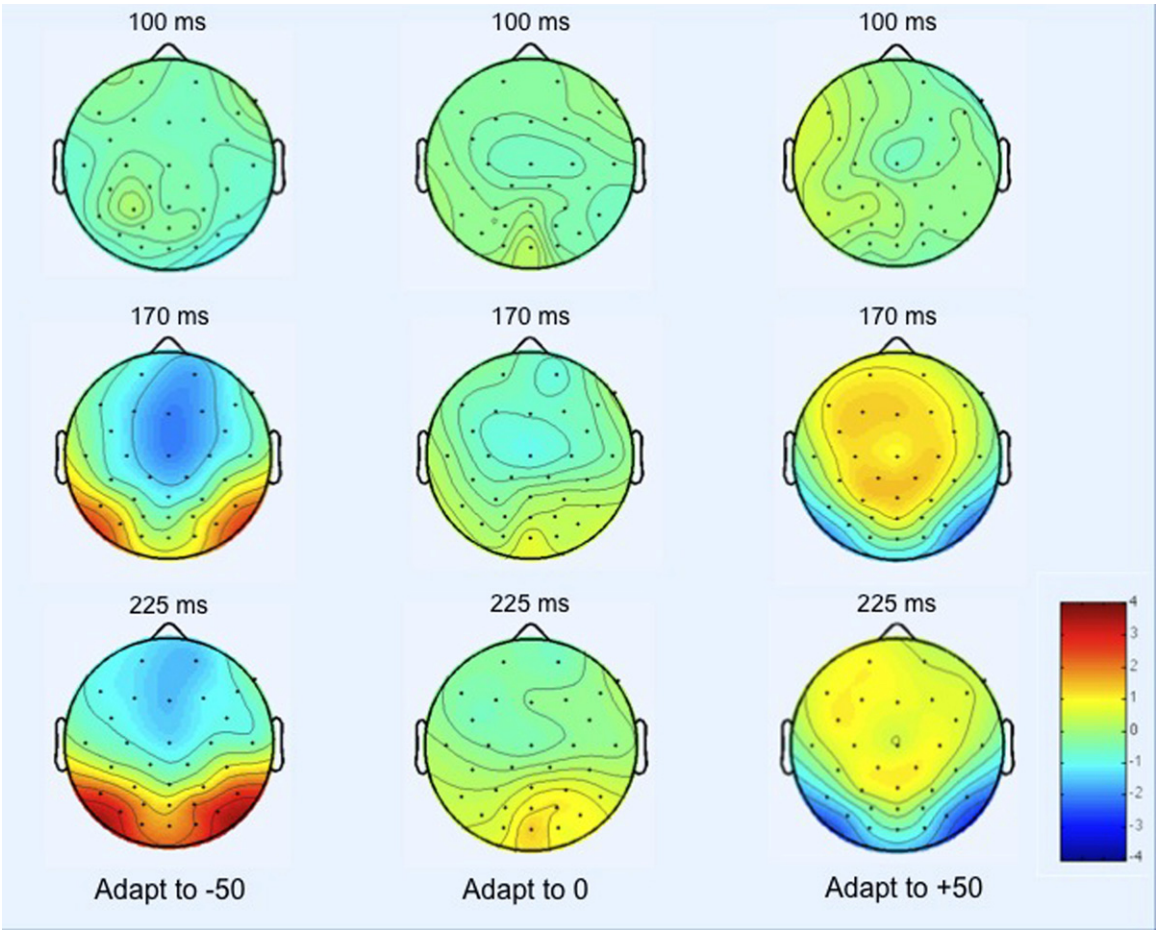

Fig. 9. Adaptation effects across the surface of the scalp for the three adaptation conditions. We subtracted the +30 distortion condition from the −30 distortion condition (equivalent to subtracting the solid line data from the dashed line data in Fig. 8) for each adaptation condition. The differences show the effect of adaptation at each electrode site. The normal face produces virtually no differential adaptation effects on the +30 and −30 distorted faces, and therefore the colors are mostly near green (zero differences). The color changes for the −50 and +50 conditions illustrate the time course, direction and extent of the adaptation effects. Color scale represents ±4 μV. (For interpretation of the references to color in this figure legend, the reader is referred to the web version of the article.)

ological correlates of perceived face distortion. Previous behavioral research demonstrated that adaptation would cause the test face to show an aftereffect in the opposite direction of the adapting condition (Webster & MacLin, 1999), and we replicated these findings with our behavioral normality ratings. The systematic modulation of the P250 ERP component by face distortion established in Experiment 1 was used in Experiment 2 to reveal both the timecourse and the directionality of the neural correlates figural aftereffects. We again observed systematic modulation of the P250 ERP component peak amplitude as a result of adapting conditions (and therefore of perceived distortion). Importantly, the direction of the modulation of the P250 peak amplitude was related to the direction of the perceived distortion: if a face was perceived to be more normal, it produced a larger P250 peak amplitude. This result is consistent with a model in which the electrophysiological correlates of adaption reflect true population coding rather than just neural fatigue. This suggests that our adaptation manipulation selectively affects a subpopulation of neurons that code a region of face space. If this adaptation cancels a physical distortion of the stimulus we see an increased normality rating and a recovery of the EEG response.

The primary support for this claim comes from the P250 ERP component in Experiment 2. The P250 peak amplitude of the −30 test face condition was lower when the preceding adapting condition of +50 was displayed. As hypothesized, the +50 adaptation condition would perceptually change the −30 test face away from the adapting condition. In other words, the −30 test face is perceived as more compressed and less normal. When the adapting condition of −50 was initially displayed, the −30 test face moved perceptually away from the adapting condition, to be perceived as more expanded and more normal. These results support that an electrophysiological substrate of figural face adaptation occurs in the P250 component.

The P250 ERP component is the earliest component to reflect figural adaptation effects modulated by different adaptation conditions. The P100 ERP component, reflecting early visual processes, showed no significant modulation by the adaptation conditions nor by face distortion itself. The N170 ERP component, thought to reflect structural encoding of faces (Bentin, Allison, Puce, Perez, & McCarthy, 1996; Itier & Taylor, 2004; Rossion & Gauthier, 2000), showed no significant modulation by the adaptation conditions, although it did exhibit a strong trend for differences between the test face distortions. This pattern is similar to previous adaptation studies which found P100 and N170 differences between adaptation and non-adaptation conditions, but no modulation of the N170 by different adaptation conditions (Kovács et al., 2006; Schweinberger et al., 2007).

3. General discussion

Our results suggest that, like facial identity, face distortion is encoded by an opponent coding process in which separate pools of

neurons code the endpoints of a continuum, and adaptation selectively fatigues at least one pool of neurons (see Regan & Hamstra, 1992; Robbins et al., 2007; Susilo et al., 2010). In an opponent coding model of figural aftereffects, expanded and compressed faces are coded along separate visual channels, or pools of neurons. We hypothesize that adaptation to expanded faces causes an attenuation of the response of the expanded face channel, which causes subsequent images to appear more compressed. For example, adaptation to a +50 face selectively attenuates the expansion pool of neurons, leaving the compression channel relatively more active. Thus, adaptation to a +50 face would cause a +30 test face to seem more compressed than it really is. Likewise, adaptation to a −50 face results in selective attenuation of the compression channel, causing a −30 test face to seem more expanded than it really is. Adaptation to a normal 0 face would attenuate both the compression and expansion channels to the same degree, which would cancel out any effect on the subsequent test face. Our behavioral and electrophysiological results fit this assertion, as adaptation to a 0 face results in no differences in ratings of perceived normality nor differences in P250 component amplitudes.

Under this opponent coding model, the magnitude of the P250 ERP component might represent the degree to which the two pools of neurons are responding approximately equally. Presentation of a normal face will result in both pools firing approximately equally, whereas a distorted face will produce an imbalance that distorts the perception of the face, resulting in a drop in the P250 component amplitude. However, adapting to the nearby distortion will selectively reduce the responding of one encoding pool of neurons, thus restoring the balance of the two pools and raising the P250 component. It has been suggested that possible mechanisms leading to this change in neural responsivity are neural fatigue, where neural activity decreases with extended exposure to the adapting stimulus, or a sharpening of the neural response tuning function, where fewer neurons respond to subsequent presentations of the adapting stimulus (Grill-Spector, Henson, & Martin, 2006). Our present results are not able to distinguish between these two possible mechanisms.

However, we believe this is the first demonstration of adaptation both increasing and decreasing the amplitude of an ERP component dependent upon whether the adaptation condition resulted in perceptions that were more or less distorted. This is consistent with the suggestion that the neural correlates of adaptation reflect genuine shifts in the neural processes that perceive distortion, rather than general fatigue in the neural system as a result of adaptation. Additionally, our observation of a crossover interaction between the adapting and test distortions supports the claim by Krekelberg, Boyton, and van Wezel (2006) that the strength of adaptation effects interacts with the type of test stimulus used to probe the adaptation, which cannot result from a simple passive fatiguing of the neurons.

The present evidence for opponent coding, together with the previous studies of figural aftereffects that are consistent with norm-based coding (Robbins et al., 2007; Susilo et al., 2010; Valentine, 1991; Webster & MacLin, 1999), suggest that one dimension of psychological face space is defined by the expanding and compressing of the spatial positions of internal face features, coded by separate pools of neurons. Furthermore, this compression-expansion dimension is reflected in both our behavioral measures of human decisions about other human faces and our scalp-level measures of neurological activity during the same tasks.

Our results are also consistent with several studies which have found that modulation of the P2 or P250 peak amplitude may reflect a dimension of normality or typicality in the representation of faces. In addition to the aforementioned Halit et al. (2000) study and our current results showing modulation of the P250 by face distortion, the P250 exhibits a larger amplitude to normal versus thatcherized faces (Milivojevic, Clapp, Johnson, & Corballis, 2003), to young versus old faces (Wiese, Schweinberger, & Hansen, 2008), and to Caucasian versus Asian (other race) faces for Caucasian observers (Stahl, Wiese, & Schweinberger, 2008). Just as adaptation modulated what was perceived as normal, which was reflected in P250 peak amplitude modulation, experience in the form of expertise with other races (Stahl et al., 2008) and normal aging (Wiese et al., 2008) also further modulates the P250 peak amplitude. We can infer that not only does the P250 reflect one possible dimension in a norm-based representation of faces, but as experience modifies our perceptual norms for faces, the P250 will reflect those shifting representations.

An alternative, though not incompatible, account for P2 amplitude modulation is offered by Aguirre and colleagues (Kahn, Harris, Wolk, & Aguirre, 2010) who demonstrated that a decrease of P2 amplitude reflects an increase in image dissimilarity. Using a carry-over ERP design (see also Drucker, Kerr, & Aguirre, 2009), they demonstrated that when two sequential images are physically more distant from each other (along an image morph sequence), the P2 amplitude is lower than when two sequential images are the same. Their results indicate that as image (physical) distance increases, P2 systematically decreases, so the P2 might reflect a neural correlate of perceived dissimilarity. In Experiment 2 of our present study, higher P250 amplitudes were observed when the test face was closer in physical image space to the adapting image (e.g., larger P250 to +30 test face in the +50 adaptation condition), consistent with an interpretation of perceived similarity. Indeed, Yamashita and colleagues (Yamashita et al., 2005) suggested that perceived similarity between faces is at least partially reflected by the selectivity of adaptation for particular stimulus dimensions. However, our results of Experiment 1 demonstrate modulation by perceived normality in a randomized presentation of images, rather than modulation by the distance between subsequent images within a sequence. Additional analyses are needed to test how much of the perceived normality modulation might be explained by perceived dissimilarity, both of which appear to be reflected along the same time course in the neural correlates of face perception.

That perceived normality or typicality and physical image similarity of faces might be reflected along the same time course, possibly by the same neural correlates, is consistent with the proposed relationship between similarity and the multidimensional model of face representation proposed by Valentine (1991). Within Valentine's framework, faces are represented by an as-yet unknown number of dimensions, where the centroid or norm of the space is an experience-defined average of all the face dimensions. Distinctive faces are those faces more distant in the multidimensional space than typical faces, and Valentine proposed that perceived dissimilarity would be one possible measure of distance in the multidimensional representation space. As adaptation recalibrates the structural encoding mechanisms, it is thought that adaptation renormalizes the representational space, shifting the norm more toward the adapting stimulus (Rhodes et al., 2003). Thus, adaptation results in a change in the distances between faces in multidimensional representation space, which would be reflected in the mechanisms reflecting changes in perceived similarity.

Our present results, together with the results of Webster and MacLin (1999), suggest that adaptation to distorted faces shifts the observer's face norm toward the distorted face, which would result in smaller distances between the norm and faces distorted in a direction similar to the adapting stimulus, and an increase in the distances between the norm and faces distorted in the direction opposite the adapting stimulus. Our P250 results reflected higher amplitude when faces were closer (more similar) to the norm and lower amplitude when faces were further (less similar)

to the norm. Thus, we have evidence that face distortion, particularly the compression/expansion of internal face features, is one possible dimension of multidimensional face representation space.

In addition to the studies of human perception that suggest face distortion is one possible dimension in a norm-based representation of faces, models of face recognition in computer vision have also extracted an internal feature compression-expansion dimension in defining a computational face space. Principal components analysis (PCA) approaches, in particular, create a face space by extracting principal components directly from the pixel information in a set of face images. Note that principal components are defined by the eigenvectors of the covariance matrix of pixel values across a set of images. Consequently, PCA-based models rely on those aspects of face images that capture a large amount of variability between faces to establish a multidimensional representation space into which all faces might be projected.[1] Importantly, each eigenvector describes the average face on that dimension, so we can visually inspect each image to see the information encoded by each principal component (Yambor, Draper, & Beveridge, 2002). One dimension extracted by PCA that accounts for a large amount of variability between natural face images is the spread of the internal face features.[2] The fact that PCA-based models extract this compression-expansion dimension as a dimension present in the naturally occurring face image statistics suggests that it is reasonable to suppose the visual system developed the machinery to code for variation along this continuum and that adaptation selectively suppresses one end of this continuum. PCA-based models provide a line of evidence convergent with human perception data that faces are likely encoded and processed within to a multidimensional representation space (Valentine, 1991).

The timing of our ERP components that are sensitive to adaptation provides some constraints on the location of the effects. We see no P100 effects due to either face distortion or figural aftereffects. We see small and inconsistent N170 effects of adaptation, and large and robust effects in the P250. Recall that the N170 has traditionally been thought to be involved with the configural processing of faces (Bentin et al., 1996; Itier & Taylor, 2004; Rossion et al., 1999). Assuming that the neural generator of the P250 component lies downstream of the generator of the N170 component, these data imply that the neurons generating the P250 are adapting to facial features at the configural level. However, it is important to note that non-face objects also elicit a smaller N170 response, and thus it is unclear whether the observed P250 effects are due to adaptation of configural mechanisms specific to face processing, or if the adaptation is affecting general purpose recognition mechanisms, such as perceived similarity. The N170/P250 complex clearly reflects a series of processes, and it is likely that early adaptation effects propagate the changes throughout the downstream mechanisms. The current demonstration of the relation between distortion and adaptation seems like a useful approach to determine the conditions under which adaptation alters the ongoing perception of stimuli.

References

Bentin, S., Allison, T., Puce, A., Perez, E., & McCarthy, G. (1996). Electrophysiological studies of face perception in humans. *Journal of Cognitive Neuroscience*, *8*, 551–565.

Bentin, S., & Deouell, L. Y. (2000). Structural encoding and identification in face processing: ERP evidence for separate mechanisms. *Cognitive Neuropsychology*, *17*, 35–54.

Busey, T. A. (n.d.). *The face machine* [*JAVA applet*]. http://cognitrn.psych.indiana.edu/nsfgrant/FaceMachine/faceMachine.html.

Carandini, M., & Ferster, D. (1997). A tonic hyperpolarization underlying contrast adaptation in cat visual cortex. *Science*, *276*, 949–952.

Delorme, A., & Makeig, S. (2004). EEGLAB: An open source toolbox for analysis of single-trial EEG dynamics including independent component analysis. *Journal of Neuroscience Methods*, *134*, 9–21.

Dragoi, V., Sharma, J., & Sur, M. (2000). Adaptation-induced plasticity of orientation tuning in adult visual cortex. *Neuron*, *28*(1), 287–298.

Drucker, D. M., Kerr, W. T., & Aguirre, G. K. (2009). Distinguishing conjoint and independent neural tuning for stimulus features with fMRI adaptation. *Journal of Neurophysiology*, *101*(6), 3310–3324.

Fang, F., & He, S. (2005). Viewer-centered object representation in the human visual system revealed by viewpoint aftereffects. *Neuron*, *45*(5), 793–800.

Gibson, J. J. (1933). Adaptation after-effects and contrast in the perception of curved lines. *Journal of Experimental Psychology*, *16*(1), 1–31.

Graham, N. (1989). *Visual pattern analyzers*. Oxford, UK: Oxford University Press.

Grill-Spector, K., Henson, R., & Martin, A. (2006). Repetition and the brain: Neural models of stimulus-specific effects. *Trends in Cognitive Sciences*, *10*(1), 14–23.

Halit, H., de Haan, M., & Johnson, M. H. (2000). Modulation of event-related potentials by prototypical and atypical faces. *NeuroReport*, *11*(9), 1871–1875.

Itier, R. J., & Taylor, M. J. (2004). N170 or N1? Spatiotemporal differences between object and face processing using ERPs. *Cerebral Cortex*, *14*(2), 132–142.

Kahn, D. A., Harris, A. M., Wolk, D. A., & Aguirre, G. K. (2010). Temporally distinct neural coding of perceptual similarity and prototype bias. *Journal of Vision*, *10*(10), 1–12.

Köhler, W., & Wallach, H. (1944). Figural aftereffects: An investigation of visual processes. *Proceedings of the American Philosophical Society*, *88*, 269–357.

Kovács, G., Cziraki, C., Vidnyanszky, Z., Schweinberger, S. R., & Greenlee, M. W. (2008). Position-specific and position-invariant face aftereffects reflect the adaptation of different cortical areas. *NeuroImage*, *43*(1), 156–164.

Kovács, G., Zimmer, M., Banko, E., Harza, I., Antal, A., & Vidnyanszky, Z. (2006). Electrophysiological correlates of visual adaptation to faces and body parts in humans. *Cerebral Cortex*, *16*(5), 742–753.

Kovács, G., Zimmer, M., Harza, I., Antal, A., & Vidnyanszky, Z. (2005). Position-specificity of facial adaptation. *Neuroreport*, *16*(17), 1945–1949.

Kovács, G., Zimmer, M., Harza, I., & Vidnyanszky, Z. (2007). Adaptation duration affects the spatial selectivity of facial aftereffects. *Vision Research*, *47*(25), 3141–3149.

Krekelberg, B., Boyton, G. M., & van Wezel, R. J. A. (2006). Adaptation: From single cells to BOLD. *Trends in Neurosciences*, *29*(5), 250–256.

Leopold, D. A., O'Toole, A. J., Vetter, T., & Blanz, V. (2001). Prototype-referenced shape encoding revealed by high-level aftereffects. *Nature Neuroscience*, *4*(1), 89–94.

Milivojevic, B., Clapp, W. C., Johnson, B. W., & Corballis, M. C. (2003). Turn that frown upside down: ERP effects of thatcherization of misorientated faces. *Psychophysiology*, *40*, 967–978.

Movshon, J. A., & Lennie, P. (1979). Pattern-selective adaptation in visual cortical neurons. *Nature*, *278*, 850–852.

Petersen, S. E., Baker, J. F., & Allman, J. M. (1985). Direction-specific adaptation in area MT of the owl monkey. *Brain Research*, *346*(1), 146–150.

Regan, D., & Hamstra, S. J. (1992). Shape discrimination and the judgment of perfect symmetry: Dissociation of shape from size. *Vision Research*, *32*, 1845–1864.

Rhodes, G., Jeffery, L., Watson, T. L., Clifford, C. W., & Nakayama, K. (2003). Fitting the mind to the world: Face adaptation and attractiveness aftereffects. *Psychological Science*, *14*, 558–566.

Rhodes, G., & Leopold, D. A. (2009). Adaptive norm-based coding of face identity. In A. J. Calder, G. Rhodes, M. H. Johnston, & J. V. Haxby (Eds.), *Handbook of face perception*. Oxford: Oxford University Press.

Robbins, R., McKone, E., & Edwards, M. (2007). Aftereffects for face attributes with different natural variability: Adaptor position effects and neural models. *Journal of Experimental Psychology: Human Perception and Performance*, *33*(3), 570–592.

Rossion, B., Delvenne, J.-F., Debatisse, D., Goffaux, V., Bruyer, R., Crommelinck, M., et al. (1999). Spatio-temporal localization of the face inversion effect: An event-related potentials study. *Biological Psychology*, *50*(3), 173–189.

Rossion, B., & Gauthier, I. (2000). How does the brain process upright and inverted faces? *Behavioral and Cognitive Neuroscience Reviews*, *1*(1), 62–74.

Schweinberger, S. R., Kloth, N., & Jenkins, R. (2007). Are you looking at me? Neural correlates of gaze adaptation. *NeuroReport*, *18*(7), 693–696.

Stahl, J., Wiese, H., & Schweinberger, S. R. (2008). Expertise and own-race bias in face processing: An event-related potential study. *NeuroReport*, *19*(5), 583–587.

Susilo, T., McKone, E., & Edwards, M. (2010). What shape are the neural response functions underlying opponent coding in face space? A psychophysical investigation. *Vision Research*, *50*(3), 300–314.

Valentine, T. (1991). A unified account of the effects of distinctiveness, inversion, and race in face recognition. *Quarterly Journal of Experimental Psychology*, *43*(2), 161–204.

Valentine, T., & Bruce, V. (1986). The effects of distinctiveness in recognizing and classifying faces. *Perception*, *15*(5), 525–535.

Webster, M. A., Kaping, D., Mizokami, Y., & Duhamel, P. (2004). Adaptation to natural facial categories. *Nature*, *428*(6982), 557–561.

Webster, M. A., & MacLin, O. H. (1999). Figural aftereffects in the perception of faces. *Psychonomic Bulletin & Review*, *6*(4), 647–653.

[1] Eigenvector dimensions defined in PCA may be considered a more objective means of defining face space, because the dimensions are extracted from the properties of the image pixels themselves.

[2] An interactive demonstration of these eigenvector face dimensions can be found in The Face Machine (Busey, n.d.), in which face distortion is the third dimension of computational face space. The Face Machine can be found online at http://cognitrn.psych.indiana.edu/nsfgrant/FaceMachine/faceMachine.html.

Wiese, H., Schweinberger, S. R., & Hansen, K. (2008). The age of the beholder: ERP evidence of an own-age bias in face memory. *Neuropsychologia*, *46*, 2973–2985.

Yamashita, J. A., Hardy, J. L., De Valois, K. K., & Webster, M. A. (2005). Stimulus selectivity of figural aftereffects for faces. *Journal of Experimental Psychology: Human Perception and Performance*, *31*, 420–437.

Yambor, W. S., Draper, B. A., & Beveridge, J. R. (2002). Analyzing PCA-based face recognition algorithms: Eigenvector selection and distance measures. In H. I. Christensen, & P. J. Phillips (Eds.), *Empirical Evaluation Methods in Computer Vision*. Singapore: World Scientific Press.

Zhao, L., & Chubb, C. (2001). The size-tuning of the face-distortion after-effect. *Vision Research*, *41*, 2979–2994.